# Negative ion photoelectron spectroscopy of the heteronuclear alkali-metal dimer and trimer anions: $NaK^-$, $KRb^-$, $RbCs^-$, $KCs^-$, $Na_2K^-$, and $K_2Cs^-$

J.G. Eaton, H.W. Sarkas, S.T. Arnold, K.M. McHugh and K.H. Bowen
*Department of Chemistry, Johns Hopkins University, Baltimore, MD 21218, USA*

Received 24 February 1992

Negative ion photoelectron spectra are reported for the heteronuclear alkali dimer and trimer anions, $NaK^-$, $KRb^-$, $KCs^-$, $RbCs^-$, $Na_2K^-$, and $K_2Cs^-$ at 488 nm. In addition to assigning all of the electronic transitions observed in the mixed dimer anion spectra, vertical detachment energies, adiabatic electron affinities, and dimer anion dissociation energies have also been determined. A linear correlation between mixed dimer $EA_a$s and $\alpha_{M^*}/r^2_{M^*M}$ ($\alpha_{M^*}$ = the more electropositive alkali atom's polarizability) confirms the presence of ionic character in heteronuclear alkali dimers. Also, vertical detachment energies and adiabatic electron affinities are reported for the trimer systems.

## 1. Introduction

Previously, we [1] reported the photoelectron spectra of the homonuclear alkali metal cluster anions: $Na^-_{n=2-5}$, $K^-_{n=2-7}$, $Rb^-_{n=2-3}$, and $Cs^-_{n=2-3}$. Here, we present the photoelectron spectra of the heteronuclear alkali-metal dimer and trimer anions: $NaK^-$, $KRb^-$, $KCs^-$, $RbCs^-$, $Na_2K^-$, and $K_2Cs^-$. Neutral heteronuclear alkali dimers [2–7] and trimers [8–11] have been the subject of several theoretical investigations. Experimental work on neutral mixed alkali dimers has included laser-induced fluorescence studies [12–19] (especially on NaK), ionization potential measurements [20], and dipole moment determinations via molecular beam electric deflection and resonance spectroscopy [21], while experimental work on neutral mixed alkali trimers has involved photoionization and abundance studies [22–25]. To our knowledge, mixed alkali-metal dimer and trimer anions had not been observed prior to the present work.

*Correspondence to:* K.H. Bowen, Department of Chemistry, Johns Hopkins University, Baltimore, MD 21218, USA.

## 2. Experimental

Negative ion photoelectron spectroscopy is performed by crossing a mass-selected beam of negative ions with a fixed frequency photon beam and energy analyzing the resultant photodetached electrons. Our spectrometer has been described previously [26]. Once negative ions are generated and extracted from their ion source, a series of ion optical components transports them through a Wien velocity filter where they are mass-selected before being focused into the field free, collision free ion/photon interaction region. There, they are crossed with the intracavity photon beam of an argon-ion laser. Some of the resulting photodetached electrons next enter the input optics of a magnetically shielded hemispherical electron energy analyzer where they are energy analyzed and counted. In the present experiment, photoelectron spectra were recorded with a photon energy of 2.540 eV, a channel spacing of 8.5 meV, and an instrumental resolution of 30 meV.

Heteronuclear alkali dimer and trimer anions were generated in a high temperature supersonic expansion ion source. In this source, the combined vapors of two alkali metals were coexpanded with 100–200 Torr of argon into high vacuum through a 200 μm

0009-2614/92/$ 05.00 

nozzle which was maintained $\approx 50\,^{\circ}C$ above the oven temperature. Relatively low energy electrons were injected into the expanding jet by a negatively biased hot filament located on the high vacuum side of the nozzle. A magnetic field was used to enhance ionization efficiency and to confine and concentrate the microplasma. Under these expansion conditions atomic, dimer, and trimer anions were the primary species observed.

## 3. Results and interpretation

The photoelectron spectra of the heteronuclear alkali dimer anions, $NaK^-$, $KRb^-$, $KCs^-$, and $RbCs^-$ are presented in fig. 1. These spectra are highly structured, individual peaks arising due to photodetachment transitions between the ground electronic states of the dimer anions and the ground and low-lying excited electronic states of their corresponding neutral dimers. All of the features observed in these spectra have been assigned, guidance having been provided by available theoretical calculations [2,27] and optical data [12,13,28,29]. Fig. 2 illustrates these assignments using the spectrum of $KCs^-$ as an example. In each mixed dimer anion spectrum, the lowest electron binding energy (EBE) feature corresponds to a photodetachment transition from the ground state of the dimer anion to the ground state ($X\,^1\Sigma^+$) of its corresponding neutral dimer, with the spectral width being a consequence of an unresolved vibrational progression. The next highest EBE feature observed in these spectra arises due to a transition to the $a\,^3\Sigma^+$ electronic state of the neutral dimer, with the spectral width in this case reflecting the slope of the largely repulsive $a\,^3\Sigma^+$ potential curve. The next major feature toward higher EBE is a relatively narrow peak, and it is due to a transition to the $A\,^1\Sigma^+$ state of the neutral dimer. The width of this feature suggests that the $A\,^1\Sigma^+$ state has an equilibrium bond length which is close to that of the dimer anion. The shoulder observed on the low EBE side of the $A\,^1\Sigma^+$ peak is due to a transition to the $b\,^3\Pi$ state. The highest EBE peak observed in the spectra of $KRb^-$, $RbCs^-$, and $KCs^-$ arises largely due to transitions to the $c\,^3\Sigma^+$ state.

Both the vertical detachment energy (VDE) and the adiabatic electron affinity ($EA_a$) were determined from the peak corresponding to the $(M\mathscr{M})$, $X\,^1\Sigma^+ + e^- \leftarrow (M\mathscr{M})^-$, $X\,^2\Sigma^+$ transition in each mixed dimer anion spectrum, where M and $\mathscr{M}$ refer to atoms of different alkali metals. The EBE of the peak maximum for this transition gave the value of VDE, while the EBE of the origin of this transition defined the value of $EA_a$. In the case of the $NaK^-$ spectrum, its origin was located initially by subtracting the $A\,^1\Sigma^+$ $(v'=0) \rightarrow X\,^1\Sigma^+$ $(v''=0)$ transition

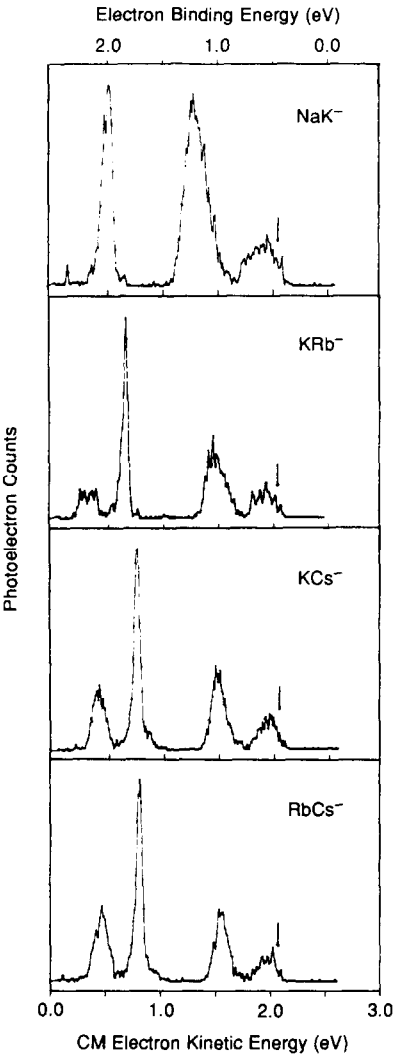


Fig. 1. The negative ion photoelectron spectra of $NaK^-$, $KRb^-$, $KCs^-$, and $RbCs^-$, each recorded using 2.540 eV photons. The arrow in each spectrum indicates our determination of the ground electronic state's origin, from which $EA_a$s were determined.

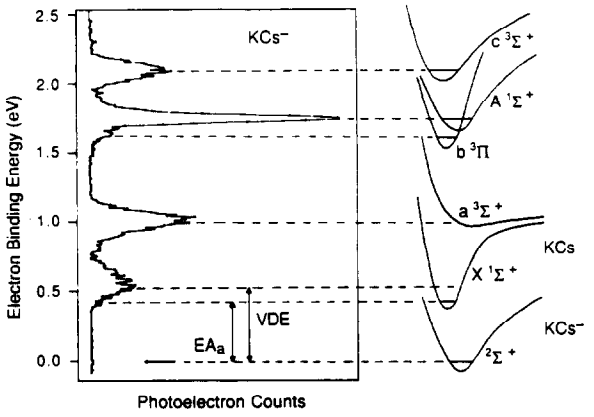


Fig. 2. Illustration of dimer transition assignments using the photoelectron spectrum of $KCs^-$ as an example.

energy of NaK [12] from the EBE of the center of the peak corresponding to the NaK, $A\,^1\Sigma^+ + e^- \leftarrow NaK^-$, $X\,^2\Sigma^+$ transition. Because the $A\,^1\Sigma^+$ $(v'=0) \rightarrow X\,^1\Sigma^+$ $(v''=0)$ transition energies of the other mixed dimers are either unknown or poorly known, the sought-after origins in their anion photoelectron spectra were located by scaling the differences between their VDE and $EA_a$ values to the widths (fwhm) of their origin-containing bands. Two choices for scale factors were provided by our previous determination of the $EA_a$ of $K_2$ and by our present determination of the $NaK^-$ origin, both using the same optical transition method described above. While scale factors from both NaK and $K_2$ electron affinity determinations gave very similar results, use of the latter supplied a more precise determination of the origins, and all mixed dimer $EA_a$ values reported in table 1 were determined by using it. With the mixed dimer $EA_a$s established, dimer anion dissociation energies, $D_0[(M\mathscr{M})^-, (X\,^2\Sigma^+)]$, were calculated using the thermochemical cycle,

$$D_0[(M\mathscr{M}), (X\,^1\Sigma^+)] + EA_a(M\mathscr{M}) = D_0[(M\mathscr{M})^-, (X\,^2\Sigma^+)] + EA_a(M)\,,$$

where $D_0[(M\mathscr{M}), (X\,^1\Sigma^+)]$ is the neutral dimer ground state dissociation energy [20], $EA_a(M\mathscr{M})$ is the adiabatic electron affinity of the mixed alkali dimer, and $EA_a(M)$ is the alkali atom adiabatic electron affinity [30]. Table 1 presents a summary of vertical detachment energies, adiabatic electron affinities, and dimer anion dissociation energies for both homonuclear and heteronuclear alkali dimer systems.

The photoelectron spectra of the heteronuclear alkali trimer anions, $Na_2K^-$ and $K_2Cs^-$ are presented in fig. 3. The $Na_2K^-$ spectrum exhibits bands due to two electronic transitions, while the $K_2Cs^-$ spectrum exhibits three. The $K_2Cs^-$ spectrum appears more complex than it actually is because of mass leakage (and thus spectral contamination) from the much more intense $KCs^-$ beam. The VDEs of $Na_2K^-$ and $K_2Cs^-$ were each determined from the peak maxima of their $(M_2\mathscr{M}), X\,^2B_2 + e^- \leftarrow (M_2\mathscr{M})^-, X\,^1\Sigma$ bands, i.e. their lowest EBE bands. The VDEs of $Na_2K^-$ and $K_2Cs^-$ were found to be $1.264 \pm 0.015$ and $1.043 \pm 0.030$ eV, respectively. Due to a substantial structural difference between neutral alkali trimers and their anions, the origin transition ener-

Table 1
Vertical detachment energies (VDE), adiabatic electron affinities ($EA_a$), and dissociation energies ($D_0$) for the homo- and heteronuclear alkali-metal dimer anions (all values in eV)

| $(M\mathscr{M})^-$ | VDE | $EA_a$ | $D_0[(M\mathscr{M})^-(X\,^2\Sigma)]$ $\{M^-(^1S)+\mathscr{M}(^2S)\}$ [a] | $D_0[(M\mathscr{M})^-(X\,^2\Sigma)]$ $\{M(^2S)+\mathscr{M}^-(^1S)\}$ [a] |
|---|---|---|---|---|
| $Na_2^-$ | $0.543 \pm 0.010$ | $0.430 \pm 0.015$ | $0.614 \pm 0.020$ | - |
| $NaK^-$ | $0.575 \pm 0.015$ | $0.465 \pm 0.030$ | $0.562 \pm 0.030$ | $0.609 \pm 0.030$ |
| $K_2^-$ | $0.550 \pm 0.010$ | $0.497 \pm 0.012$ | $0.510 \pm 0.020$ | - |
| $KRb^-$ | $0.579 \pm 0.015$ | $0.486 \pm 0.020$ | $0.480 \pm 0.020$ | $0.495 \pm 0.020$ |
| $Rb_2^-$ | $0.537 \pm 0.010$ | $0.498 \pm 0.015$ | $0.498 \pm 0.020$ | - |
| $KCs^-$ | $0.547 \pm 0.015$ | $0.471 \pm 0.020$ | $0.436 \pm 0.020$ | $0.465 \pm 0.020$ |
| $RbCs^-$ | $0.531 \pm 0.015$ | $0.478 \pm 0.020$ | $0.464 \pm 0.020$ | $0.478 \pm 0.020$ |
| $Cs_2^-$ | $0.511 \pm 0.010$ | $0.469 \pm 0.015$ | $0.447 \pm 0.020$ | - |

[a] Products of dissociation.

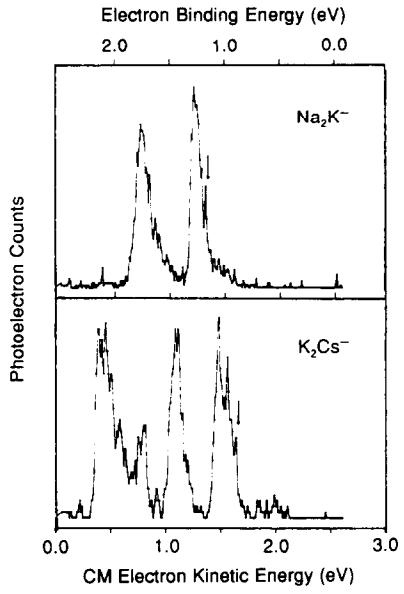


Fig. 3. The negative ion photoelectron spectra of $Na_2K^-$ and $K_2Cs^-$, each recorded using 2.540 eV photons. The arrow in each spectrum indicates our determination of the ground electronic state's origin, from which $EA_a$s were determined.

gies in their photoelectron spectra may differ significantly from their VDEs. Previously, in our studies of homonuclear alkali trimer anions, we assigned the origin transition in each photoelectron spectrum to the abrupt change in slope observed on the low EBE side of the origin-containing band. The details of this procedure were supported by theoretical calculations [31] on $Na_3$ and $K_3$ which estimated in each case the energy difference between the neutral in its ground state geometry and the neutral in the geometry of its anion. This approximated the energy differences between the VDE and the $EA_a$ for those species, from which their origins were determined. Here, we have located the origins in the spectra of $Na_2K^-$ and $K_2Cs^-$ by scaling the differences between their VDEs and their $EA_a$s to the widths of their origin-containing peaks and utilizing scale factors provided by our previous determinations of $EA_a$s for homonuclear alkali trimers. This procedure has yielded $EA_a$s of $1.167 \pm 0.050$ and $0.900^{+0.060}_{-0.040}$ eV for $Na_2K$ and $K_2Cs$, respectively.

## 4. Discussion

Here, we compare the properties of homonuclear and heteronuclear alkali dimers in terms of their electronic structures and their adiabatic electron affinities. Fig. 4 summarizes the periodic trend in electronic state splittings for both homonuclear and heteronuclear neutral alkali dimers (at the geometries of their corresponding dimer anions). In each case, these splittings represent the energy differences between the peak maxima in its anion's photoelectron spectrum, with the peak maximum of the lowest EBE transition defined as zero (ground state) energy. For the most part, the magnitudes of these splittings decrease with increasing dimer mass, and those of the heteronuclear dimers lie between those of their corresponding homonuclear dimers. The $A\,^1\Sigma^+$–$X\,^1\Sigma^+$ splittings of the heteronuclear dimers tend to be closer in energy to the $A\,^1\Sigma^+$–$X\,^1\Sigma^+$ splittings of the heav-

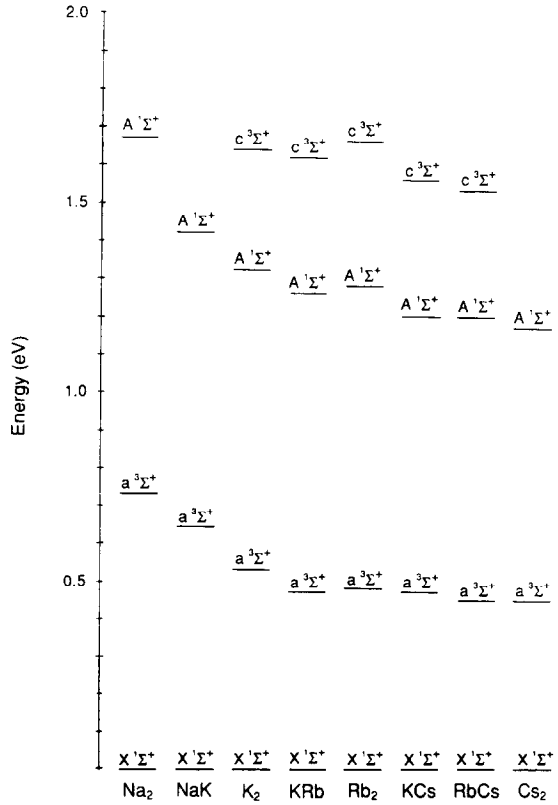


Fig. 4. The periodic trend in electronic state splittings for both homonuclear and heteronuclear neutral alkali dimers (at the geometries of their corresponding dimer anions).

ier of their corresponding homonuclear dimers. Essentially, this is because the $A\,^1\Sigma^+$ states of the heteronuclear dimers arise from the $^2S$ state of the lighter alkali atom and the $^2P$ state of the heavier atom, the $^2P$ state for the heavier of the alkali atoms being lower in energy than that of the lighter one. The decrease in $A\,^1\Sigma^+$–$X\,^1\Sigma^+$ splittings is greatest in going from $Na_2$ to NaK to $K_2$ and becomes more gradual among the heavier alkali dimers, mimicking the periodic behavior of alkali atom $^2P$–$^2S$ state separations from sodium through cesium.

Calculations by Partridge et al. [32] predicted the ordering of homonuclear alkali dimer $EA_a$s to be $Na_2 < K_2 \sim Rb_2 > Cs_2$, a result which was confirmed in our subsequent photoelectron studies of their anions [1]. Fig. 5a summarizes the periodic trend in $EA_a$s among both homonuclear and heteronuclear alkali dimers. The $EA_a$s of the mixed dimers tend to fall between the $EA_a$s of their corresponding homonuclear dimers, in quantitative agreement with the predictions of the interpolation procedure developed by Cavaliere et al. [7] for estimating spectroscopic constants of asymmetric alkali dimers.

While heteronuclear and homonuclear alkali dimers are similar chemically, they differ in an important respect, the former have non-zero dipole moments and the latter do not. Dipole moment measurements led Dagdigian and Wharton [21] to interpret the bonding in mixed alkali dimers in terms of an ionic model. The anions of ionic diatomics have been studied by Lineberger and co-workers [33], who found a linear correlation between the $EA_a$s of alkali halides (MX) and $\alpha_M/r_{MX}^2$, where $\alpha_M$ is the alkali atomic polarizability and $r_{MX}$ is the internuclear separation. This was rationalized in terms of the excess electron of the anion residing in an alkali-centered orbital which in turn is polarized away from the adjacent halide anion, i.e., $X^-...(M^+e^-)$. We have applied their model for the stability of the anions of ionic diatomics to heteronuclear alkali dimer anions. Fig. 5b shows a good correlation between the $EA_a$s of mixed alkali dimers and $\alpha_{M*}/r_{M*M}^2$, where in each case $\alpha_{M*}$ is the polarizability of the more electropositive alkali atom [#1]. This reveals the presence of ionic character in the heteronuclear alkali dimers and

[#1] An analogous plot for the homonuclear dimers gave only scattered points.

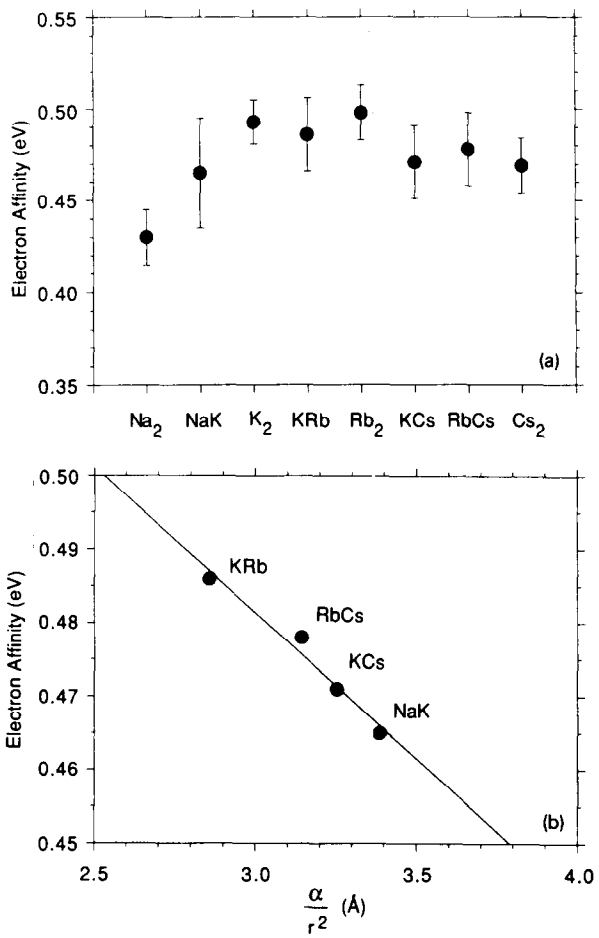


Fig. 5. (a) The periodic trend in adiabatic electron affinities for the homonuclear and heteronuclear alkali dimers. (b) Plot of heteronuclear alkali dimer electron affinities versus $\alpha_{M*}/r_{M*M}^2$, where in each case $\alpha_{M*}$ is the polarizability of the more electropositive alkali atom.

is consistent with previous work [21]. Interestingly, the periodic presentation in fig. 5a fails to show any obvious effect due to mixed dimer dipole moments.

## Acknowledgement

We thank D. Patel-Misra for help with some of the experiments and Paul Dagdigian for stimulating discussions. We gratefully acknowledge the support of ARCO Chemical Company and the National Science Foundation under grant No. CHE 9007445.

## References


[1] K.M. McHugh, J.G. Eaton, G.H. Lee, H.W. Sarkas, L.H. Kidder, J.T. Snodgrass, M.R. Manaa and K.H. Bowen, J. Chem. Phys. 91 (1989) 3792.

[2] W.J. Stevens, D.D. Konowalow and L.B. Ratcliff, J. Chem. Phys. 80 (1984) 1215.

[3] B. Bussery, Y. Achkar and M. Aubert-Frecon, Chem. Phys. 116 (1987) 319.

[4] G.H. Jeung, J.P. Daudey and J.P. Malrieu, Chem. Phys. Letters 94 (1983) 300.

[5] P. Habitz, W.H.E. Schwarz and R. Ahlrichs, J. Chem. Phys. 66 (1977) 5117.

[6] R. Janoschek and H.U. Lee, Chem. Phys. Letters 58 (1978) 47.

[7] P. Cavaliere, G. Ferrante and L. LoCascio, J. Chem. Phys. 62 (1975) 4753.

[8] S.C. Richtsmeier, M.L. Hendewerk, D.A. Dixon and J.L. Gole, J. Phys. Chem. 86 (1982) 3932.

[9] B.K. Rao and P. Jena, Phys. Rev. B 37 (1988) 2867.

[10] A.J.C. Varandas, V.M.F. Morias and A.A.C.C. Pais, Mol. Phys. 58 (1986) 285.

[11] B.K. Rao and P. Jena, Intern. J. Quantum Chem. 22 (1988) 287.

[12] A.J. Ross, R.M. Clements and R.F. Barrow, J. Mol. Spectry. 127 (1988) 546, and references therein.

[13] A.J. Ross, C. Effantin, J. d'Incan and R.F. Barrow, Mol. Phys. 56 (1985) 903.

[14] A.J. Ross, C. Effantin, J. d'Incan and R.F. Barrow, J. Phys. B 19 (1986) 1449.

[15] D. Eisel, D. Zevgolis and W. Demtroder, J. Chem. Phys. 71 (1979) 2005.

[16] E.J. Breford and F. Engelke, J. Chem. Phys. 71 (1979) 1994.

[17] E.J. Breford and F. Engelke, Chem. Phys. Letters 53 (1978) 282.

[18] R. Beuc, S. Milosevic and G. Pitchler, J. Phys. B 17 (1984) 739.

[19] T. Gustavsson, C. Amiot and J. Verges, Chem. Phys. Letters 143 (1988) 101.

[20] M.M. Kappes, M. Schar and E. Schumacher, J. Phys. Chem. 89 (1985) 1499.

[21] P.J. Dagdigian and L. Wharton, J. Chem. Phys. 57 (1972) 1487.

[22] E.J. Robbins, R.E. Leckenby and P. Willis, Advan. Phys. 16 (1967) 739.

[23] P.J. Foster, R.E. Leckenby and E.J. Robbins, J. Phys. B 2 (1969) 478.

[24] A. Herrmann, E. Schumacher and L. Woste, J. Chem. Phys. 68 (1978) 2327.

[25] M.M. Kappes, M. Schar and E. Schumacher, J. Phys. Chem. 91 (1987) 658.

[26] J.V. Coe, J.T. Snodgrass, C.B. Freidhoff, K.M. McHugh and K.H. Bowen, J. Chem. Phys. 84 (1986) 618.

[27] D.D. Konowalow and M.E. Rosenkrantz, in: Metal bonding and interactions in high temperature systems, eds. J.L. Gole and W.C. Stwalley (American Chemical Society, Washington, 1982) p. 3.

[28] M.E. Kaminsky, J. Chem. Phys. 66 (1977) 4951.

[29] A.J. Ross, P. Crozet, C. Effantin, J. d'Incan and R.F. Barrow, J. Phys. B 20 (1987) 6225.

[30] H. Hotop and W.C. Lineberger, J. Phys. Chem. Ref. Data 4 (1975) 539.

[31] T.C. Thompson, G. Izmirlian Jr., S.J. Lemon, D.G. Truhlar and C.A. Mead, J. Chem. Phys. 82 (1985) 5597.

[32] H. Partridge, D.A. Dixon, S.P. Walch, C.W. Bauschlicher Jr. and J.L. Gole, J. Chem. Phys. 79 (1983) 1859.

[33] T.M. Miller, D.G. Leopold, K.K. Murray and W.C. Lineberger, J. Chem. Phys. 85 (1986) 2368.